Mixed Dimer Double-Resonance Substrates for Surface-Enhanced Raman Spectroscopy

Mohamad G. Banaee* and Kenneth B. Crozier*

School of Engineering and Applied Sciences, Harvard University, Cambridge, Massachusetts 02138, United States

ARTICLE

ABSTRACT Surface-enhanced Raman spectroscopy is performed on pairs of gold nanoparticles, for which the nanoparticles in each pair have different shapes. The dimers therefore exhibit two plasmon resonances. These structures, termed mixed dimer double-resonance substrates, enable strong field enhancement at pump and Stokes frequencies in surface-enhanced Raman spectroscopy. The extinction spectra of mixed dimers are measured and simulated to identify their plasmon resonances. The experimentally determined enhancement factors of double-resonance structures are compared to those of single-resonance substrates.

KEYWORDS: double-resonance SERS substrate · surface plasmon polariton · surface-enhanced Raman scattering · heterodimers · metal nanoparticles · hyper-Raman scattering

The localized surface plasmon resonances (LSPRs) of noble metal nanoparticles strongly depend on their shape, size, arrangement, and, for pairs of closely spaced nanoparticles, the width of the gaps between them.[1,2] The ability of metallic nanoparticles to produce enormous near-field enhancements offers a sensitive tool to enhance spectroscopic signals of molecules attached to their surfaces. In surface-enhanced Raman spectroscopy (SERS) the field enhancement accompanying LSPR boosts the normally small Raman cross-section of molecules by several orders of magnitude.[3,4] SERS substrates often have a dominant LSPR peak with a bandwidth on the order of 100 nm, sufficiently wide to provide enhancement at the frequencies of the excitation laser and the Stokes Raman vibrational modes, as long as these are relatively close together. The enhancement factor in SERS is proportional to the product of the intensity enhancement at the laser frequency by that at the Raman scattering frequency. McFarland *et al.* found that the maximum SERS enhancement occurs at excitation wavelengths slightly shorter than the LSPR wavelength, such that both the incident photon and the Raman scattered photon are strongly enhanced.[5]

Recently, double-resonance substrates with plasmon resonances at the laser excitation and Raman scattering frequencies were demonstrated, and it was shown that they offer higher enhancement than similar structures with single resonances.[6] In that work, the double resonances resulted from the hybridization of LSPRs of metal nanoparticles in an array, and the surface plasmon polariton on a gold film separated from the nanoparticles by a spacer layer.[7,8] Here, we demonstrate a different means to achieve double resonances through the use of mixed dimers: pairs of nanoparticles with different shapes and plasmon frequencies.

Phenomena analogous to electromagnetically induced transparency (EIT) have been demonstrated by coherent coupling between pairs of metal nanoparticles with similar resonance frequencies.[9] To observe this effect, one mode (bright resonance) is directly excited by the incident light, but the second mode (dark plasmonic resonance) radiates by coupling to the first mode[10] and the destructive interference between them leads to the EIT effect. In addition, in structures with broken symmetry, the interaction between narrow dark modes and broad bright modes results in Fano line-shape responses.[11] Here, by contrast, we study the interaction of two bright LSPR modes with different resonance frequencies. We operate in a weak coupling regime, with the presence of one nanoparticle having only a minor influence on the resonance wavelength of the other.

In this work, we compare the SERS enhancement factors of double-resonance substrates to those of single-resonance substrates. Double-resonance substrates are formed for which there is strong spatial

*Address correspondence to mbanaee@seas.harvard.edu, kcrozier@seas.harvard.edu.

Received for review October 12, 2010 and accepted December 02, 2010.

Published online December 16, 2010. 10.1021/nn102726j

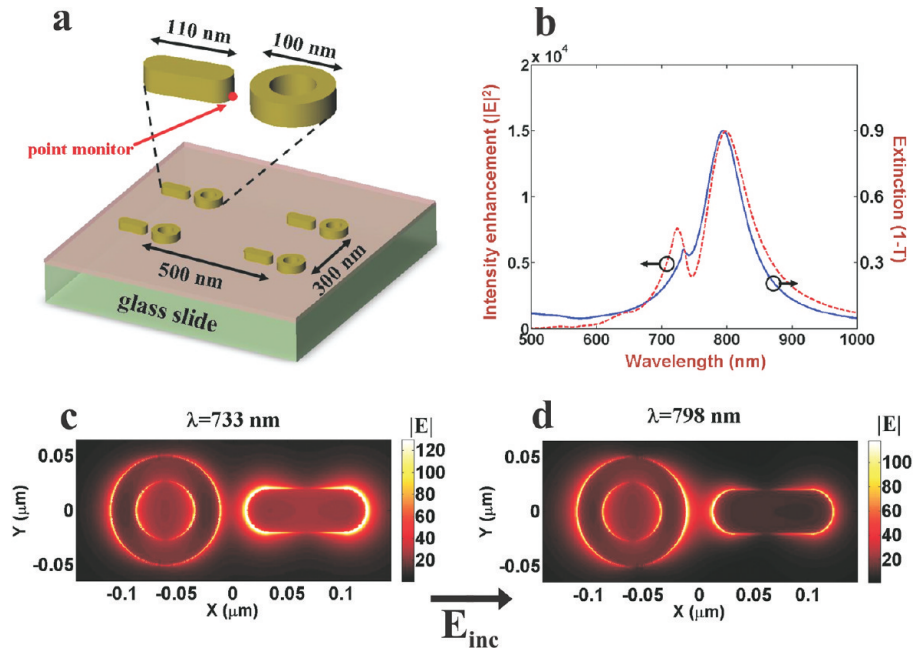

Figure 1. (a) Schematic of the mixed dimer structure. Four unit cells are shown. (b) Simulated extinction (solid line) and near-field intensity (dashed line) spectra. Near-field intensity spectrum shows intensity enhancement at a monitor point on the rod as a function of illumination wavelength. Near-field spectrum exhibits two pronounced resonances at λ = 733 and 798 nm. (c) Normalized field distribution, $|E|$, for illumination at λ = 733 nm and (d) for illumination at λ = 798 nm.

overlap between the hot spot regions at the two frequencies. In addition, double-resonance substrates are formed for which the overlap is weak. This allows us to study the role of the spatial overlap between the enhanced field at pump and Raman Stokes frequencies on the SERS enhancement. It is shown that the flexibility to tune the peak separation in a double-resonance structure improves the field enhancements of Stokes components far from the laser line. This property offers a way to increase the bandwidth of SERS, enabling it to be used for Raman lines with longer wavenumbers. In addition to conventional SERS, we anticipate that the double-resonance substrate we introduce here will be useful for increased field enhancement in surface-enhanced hyper-Raman scattering[12] and surface-enhanced second harmonic generation.[13] In those cases, the two resonances should be located at ω and 2ω. Since Raman and hyper-Raman scattering have different selection rules, they offer a complementary method to map the vibrational modes of the molecule under study.[14]

The mixed dimer SERS substrates we investigate have double resonances about λ = 800 nm. These consist of two-dimensional arrays of pairs of particles, where each pair consists of a rod and a ring. The optical near- and far-fields of the dimers are calculated numerically. Extinction and SERS measurements are carried out. For comparison, double dimer substrates are investigated. These substrates comprise arrays of pairs of rods ("rod dimers") and pairs of rings ("ring dimers"). The rod and ring dimers have different resonance frequencies, meaning that the extinction spectrum exhibits double plasmon resonances, as determined from the transmission of the entire array. Finally, the SERS enhancement factors of the above structures are compared to single-resonance substrates that consist of arrays of rod dimers.

NUMERICAL SIMULATIONS

We begin with electromagnetic simulations of the dimer structures. Figure 1a shows the schematic of the gold mixed dimer pattern. The substrate is glass, onto which a 20 nm thick layer of indium tin oxide (ITO) is deposited. ITO refractive index is taken as 1.65.[15] The dimensions of the simulated structures are chosen to match those of the fabricated structures, as determined by scanning electron microscopy (SEM). The lattice is a rectangular array with a period of 500 nm along the dimer axis and 300 nm along the perpendicular direction. The inner and outer diameters of the rings are 55 and 100 nm, respectively. The rods are 110 nm long and 40 nm wide and have tips with radii of 20 nm. The rod and ring nanoparticles are separated by gaps of 25 nm and are 30 nm thick.

The finite difference time domain (FDTD) method is used to simulate the optical response of the dimer structures. A plane wave illuminates the structure from the glass side at normal incidence, with the incident field ("E_{inc}" of Figure 1 panels c and d) polarized along the dimer axis. A square grid with a spacing of 0.5 nm along the *x*, *y*, and *z* directions is used. To make sure that our calculations properly converge at this mesh

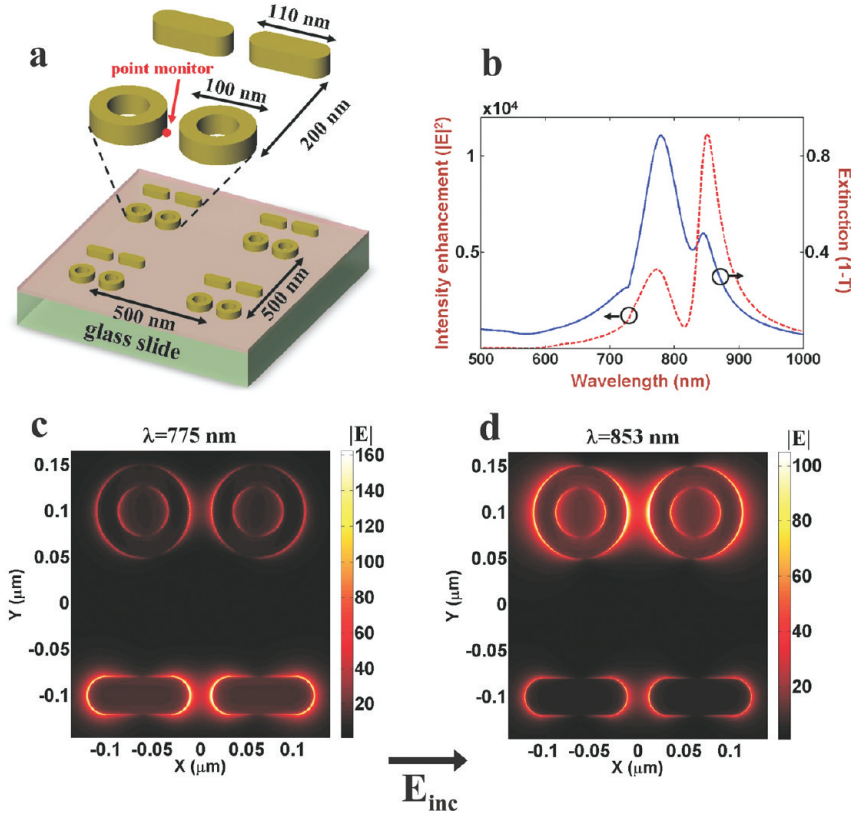

Figure 2. (a) Double dimer substrate. (b) Simulated extinction (solid line) and near-field intensity spectrum (dashed line) of the structure, with resonances at λ = 775 and 853 nm. (c) Normalized field distribution, |*E*|, for illumination at λ = 775 nm, and (d) the field distribution for illumination at λ = 853 nm.

size, we repeat the calculation with a grid spacing of 0.25 nm. The resonance wavelength and peak intensity enhancement vary by only ~0.1% and ~4%, respectively. The FDTD software (Lumerical Solutions, Inc.) models the gold dielectric response using the experimental data of Johnson and Christy.[16] In Figure 1b, we plot the simulated extinction spectrum (solid line) of the mixed dimer, which shows a double-resonance response. The near-field intensity (dashed line) spectrum of the structure at a point on the rod surface is obtained. The position of the point monitor is indicated in Figure 1a. Two peaks can be seen at wavelengths of 733 and 798 nm. In Figure 1b, the near-field intensity is the square of the electric field ($|E|^2$) at the monitor point on the rod surface, normalized to that of the incident intensity at the same location in the absence of gold particles. As discussed above, the appropriate choice of the dimensions of the rod and ring enables the shorter wavelength resonance to be matched to the laser excitation wavelength, and the longer wavelength resonance to be matched to the Stokes Raman wavelength. Figure 1 panels c and d show the field distribution on the bottom surface of the dimer structures, that is, at the gold−glass interface. These plots are the magnitude of the electric field (|*E*|) normalized to the electric field produced by the incident illumination in the absence of the dimers.

The double dimer substrate, Figure 2a, consists of a two-dimensional square array of rod and ring dimers. The unit cell consists of a rod dimer positioned adjacent to a ring dimer, with a center-to-center spacing of 200 nm. The unit cell is repeated with a period of 500 nm along both axes. The gap, thickness, and dimensions of the rod and ring nanoparticles are the same as those of the mixed dimers. The extinction spectrum and the normalized intensity spectrum, at a point on the ring surface shown in Figure 2a, are plotted in Figure 2b. The field distributions on the bottom surface of the dimers, that is, at the gold−glass interface, are shown as Figure 2 panels c and d for illumination at λ = 775 nm and λ = 853 nm, respectively. As before, these show the electric field (|*E*|) normalized to that of the incident illumination. For both mixed and double dimers, plane wave illumination at a wavelength corresponding to that of the shorter wavelength resonance leads to enhancement around the rods. Similarly, illumination at a wavelength corresponding to that of the longer wavelength resonance leads to enhancement around the rings.

In our SERS experiments, we form benzenethiol monolayers that cover all of the exposed gold surfaces of the dimers. From the measured SERS spectra, we obtain the enhancement factor (EF), which represents the factor by which the Raman scattering from the benzenethiol has been increased by the nanostructures, as

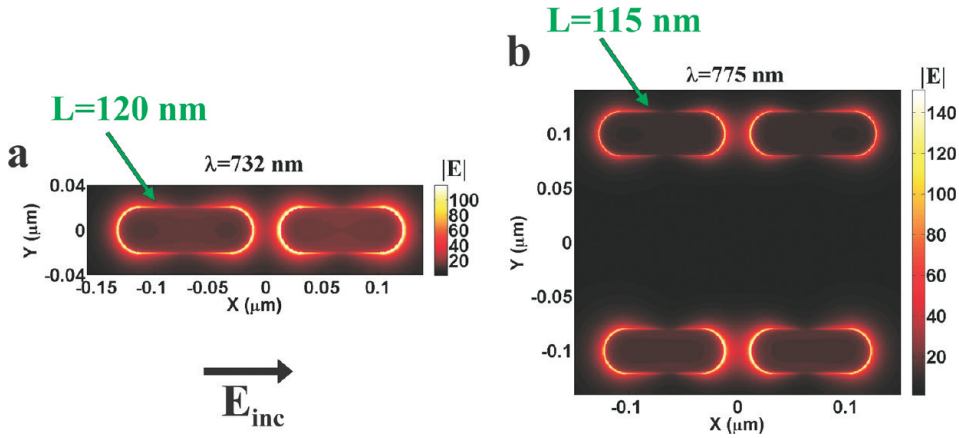

Figure 3. Normalized field distribution $|E|$ for illumination at high frequency peak of the double-resonance substrates for (a) mixed dimers of rods with different lengths and (b) double dimers of rods with different lengths.

compared to benzenethiol molecules in pure liquid form. The enhancement factor obtained in this way represents an average. Because of the wide variation in field enhancement over the substrate, some molecules likely experience far greater EF than this average value.[17] It is generally acknowledged that SERS enhancement is due to electromagnetic and chemical mechanisms.[3] To simulate the average SERS enhancement factor due to electromagnetic effects, we integrate $|E(\lambda_{ex})|^2|E(\lambda_S)|^2$ over all exposed surfaces of the dimers, that is, over the wall and top surfaces, and divide it by the surface area. Here λ_{ex}, is the excitation wavelength and λ_S is the Stokes Raman line wavelength shifted by $\sim$1074 cm^{-1}. The average simulated SERS enhancements due to electromagnetic effects for the mixed and double dimers are 2.7×10^4 and 1.6×10^4, respectively. From Figures 1 and 2, it can be seen that the peak field enhancements are higher for the double dimer than the mixed dimer. On the other hand, the double dimer average EF is only roughly half that of the mixed dimer. This is due to the poorer spatial overlap between the field distributions at the laser and Stokes wavelengths in the double dimer case.

In the geometries we considered so far, double resonances are obtained by nanoparticles with different shapes, and hence different resonance frequencies. Double-resonance responses can also be obtained by rod dimers comprising rods with different lengths. Figure 3a shows a mixed dimer of rods, in which the left and right rods are 120 and 110 nm long, respectively. This structure has a double-resonance with the high frequency peak centered at 732 nm. It can be seen that the field enhancement ($|E|_{max} = 119$) around the 110 nm long rod in the rod dimer is smaller than that around the 110 nm long rod in the mixed dimer (Figure. 1c, $|E|_{max} = 129$). A similar situation occurs for the double dimers of rods. For these, the unit cell comprises a pair of rods, each 115 nm long, at the top, and a pair of rods, each 110 nm long, on the bottom (Figure. 3b). The peak enhancement around the 110 nm long rods ($|E|_{max} = 151$) is again smaller than the peak enhancement (Figure 2c, $|E|_{max} = 162$) around the 110 nm long rods of the double dimer substrates having pairs of rings and pairs of rods. We believe this is due to the bigger physical cross section of ring particles as compared to to that of the rod particles. This enables them to concentrate the incident light more efficiently on the rod nanoparticles, in a manner analogous to a nanolens.[18−20]

RESULTS AND DISCUSSION

To demonstrate the control of the plasmon resonance spectrum enabled by the mixed and double dimers, structures similar to those of Figure 4 are fabri-

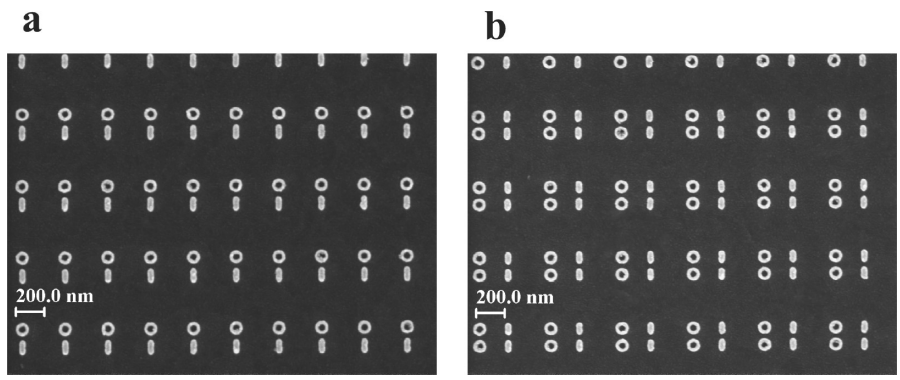

Figure 4. SEM images of fabricated substrates: (a) mixed dimer structures. (b) double dimer structures.

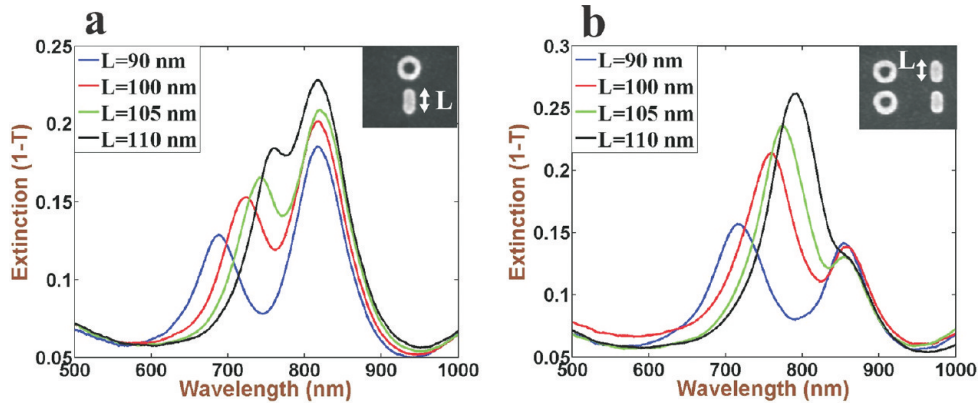

Figure 5. Measured extinction spectra of (a) mixed dimer, (b) double dimer geometries. The rod length is denoted by L.

cated with rod lengths ranging from 90 to 110 nm. The inner and outer diameters of the rings are kept fixed at 55 and 100 nm, respectively. White light transmission spectroscopy is performed to determine the plasmon resonance wavelengths of the fabricated structures. Light from a tungsten halogen lamp is collimated and polarized, and illuminates the sample at normal incidence. The transmitted light is collected into a spectrometer. The transmitted spectra are normalized to the spectra from an unpatterned region of the substrate to find the normalized transmission, *T*. The extinction is found as $(1 - T)$, with the result shown in Figure 5a,b. As shown in Figure 5, by increasing the length of rods from 90 to 110 nm, the shorter wavelength resonance gradually moves toward the longer wavelength resonance.

A monolayer of benzenethiol is then formed on the samples. The samples are vertically immersed in a 3 mM solution of benzenethiol in ethanol for 2 h. The samples are then gently washed in ethanol for 30 s and blown dry with nitrogen gas. SERS measurements are carried out using a confocal Raman microscope. Light is focused onto the sample with an objective lens with a numerical aperture of 0.4. For both the mixed and double dimers, the optical power incident on the substrate is 500 μW. The use of a tunable laser (continuous wave Ti-Sapphire) enables the illumination wavelength to be chosen to match the position of the shorter wavelength resonance of the substrate. For the double dimer substrate, $\lambda = 770$ nm is used, while $\lambda = 740$ nm is used for the mixed dimers. In Figure 6a,b, the extinction spectra of the mixed and double dimers with rod lengths of 110 nm are shown again, with the wavelengths of the laser and the Raman line of benzenethiol at 1074 cm^{-1} given by dashed lines. It can be seen that these match the plasmon resonances of these substrates well. The SERS spectra obtained for double dimer and mixed dimer structures with rod lengths of 110 nm are shown in Figure 6c.

To determine the SERS enhancement factor, the measured SERS signal is compared to that measured on a sample of neat benzenethiol, taking into account the number of molecules in each case.[21] For the SERS substrates, the number of molecules is determined by multiplying the packing density of benzenethiol by the area of the exposed surfaces of the nanoparticles. For the neat benzenethiol case, the collection volume of the confocal microscope is measured. This is performed by measuring the Raman signal from a silicon wafer as a function of position as it is translated along the optical axis.[21] The enhancement factor is then determined to be 7.2×10^6 for the mixed dimer and 1.7×10^6 for the double dimer geometries for the benzenethiol vibrational mode at 1074 cm^{-1}. The mixed dimer substrate shows a roughly 4-fold larger SERS enhancement than the double dimer geometry. The difference in the SERS enhancement factor of these two geometries is 2-fold in the numerical calculation. It may be possible that the differences between simulations and experiment are due to fabrication imperfections.

The ability of the mixed dimer substrates to provide enhancement at laser and Stokes wavelengths becomes increasingly advantageous for Stokes vibrational modes far from the laser line. To show this, SERS measurements are carried out on 1,4-phenylene diisocyanide (1,4-PDI) molecules,[22,23] using mixed dimers, and with rod dimer substrates with single resonances. This molecule has relatively strong SERS lines at 1165, 1602, and 2175 cm^{-1}. A periodic array of rod dimers with each rod 110 nm long, gaps of 25 nm between rods, and a periodicity of 500 nm along the dimer axis and 300 nm along the perpendicular direction is fabricated. An SEM image of the rod dimer substrate is shown in the inset of Figure 7b. In addition, a mixed dimer substrate with the same periodicity, gap separation, and rod length as Figure 1a, but with rings with different dimensions is made. The inner and outer diameters of the rings are 65 and 110 nm, respectively. With the new ring diameter, the peak of the second resonance is separated from the first peak by ~2200 cm^{-1}. To show the efficiency of these substrates at detecting

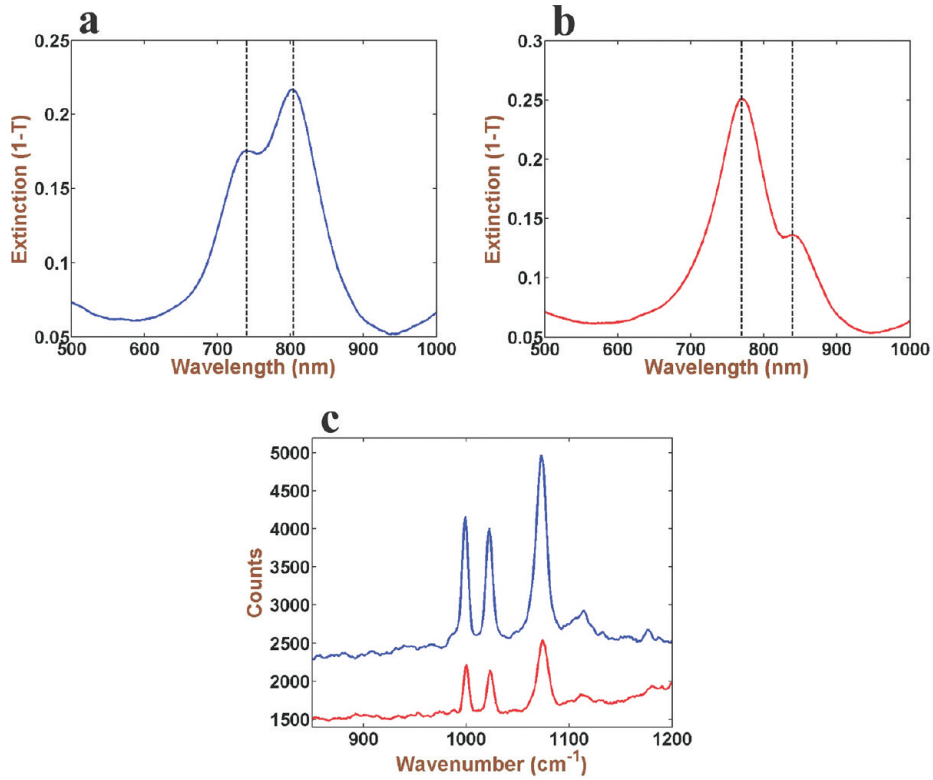

Figure 6. (a) Extinction spectrum of mixed dimers (L = 110 nm) and (b) extinction spectrum of double dimers (L = 110 nm). Dashed line show the wavelengths of the laser and of the benzenethiol Raman signal at 1074 cm^{-1}. (c) SERS spectra of a self-assembled monolayer of benzenethiol covering the double dimer (red line) and mixed dimer (blue line) substrates.

the Stokes Raman signal at 2175 cm^{-1}, SERS measurements are carried out. For the mixed dimer substrate, the laser wavelength is tuned to 760 nm. In Figure 7a, the extinction spectrum of the mixed dimer substrate is shown, along with the positions of the laser wavelength and of the Raman lines at 1165, 1602, and 2175 cm^{-1}. For the rod dimers, SERS spectra are recorded at laser wavelengths of 716 and 781 nm. In Figure 7b, the extinction spectrum of the rod array is shown, along with the laser and Raman lines for illumination at 716 nm. In this case the LSPR peak is roughly midway between the excitation and Raman line at 2175 cm^{-1}. In Figure 7c, the extinction spectrum is shown, with the positions of the laser and Raman lines for illumination at 781 nm, the plasmon resonance extinction peak wavelength.

Self-assembled monolayers of 1,4-PDI are formed by soaking the substrates in a 4 mM solution of 1,4-PDI in methanol for 3 h, rinsing them in methanol, and blowing them dry with nitrogen gas. SERS spectra are then recorded with laser excitation at 760 nm for the mixed dimers, and at 716 and 781 nm for the rod array. The results are shown in Figure 7d. The Raman line at 1165 cm^{-1} for 716 nm excitation is missing due to the fact that a 785 nm long pass filter is used in the SERS measurement, which blocks this Raman line. The spectrum of the mixed dimer substrate is obtained with a laser power of 1.3 mW incident upon the substrate. The rod array spectra are obtained with 1.1 mW laser power incident on the sample. In addition, due to the differences in the areas of the exposed gold surfaces of the structures, the numbers of molecules in the laser spot are different for the mixed and rod dimers. To facilitate comparison between these spectra, the fluorescent baseline is first removed from the SERS spectra of Figure 7d and the rod dimer spectra are then divided by a factor that accounts for the differences in powers and exposed gold surfaces. Namely, the spectra of rod dimers are divided by the ratio of the optical power used in measuring their spectra to that used in the mixed dimer case, and by the ratio of the number of molecules in the laser spot for the rod dimer case to that in the mixed dimer case. The result is shown in Figure 7e. From this Figure, the relative enhancement factors of the substrates can be found. This requires measurement of Raman signals from a reference sample, a ~10 mM solution of the 1,4-PDI molecules in methanol, at each excitation wavelength used in the SERS measurement. The peaks of the SERS spectra of Figure 7e are normalized to the corresponding peaks of the reference Raman spectra. The results are shown in Table 1. Comparison of the signal strengths of Table 1 enables the relative enhancement factors of the mixed dimer and rod dimer substrates to be found.

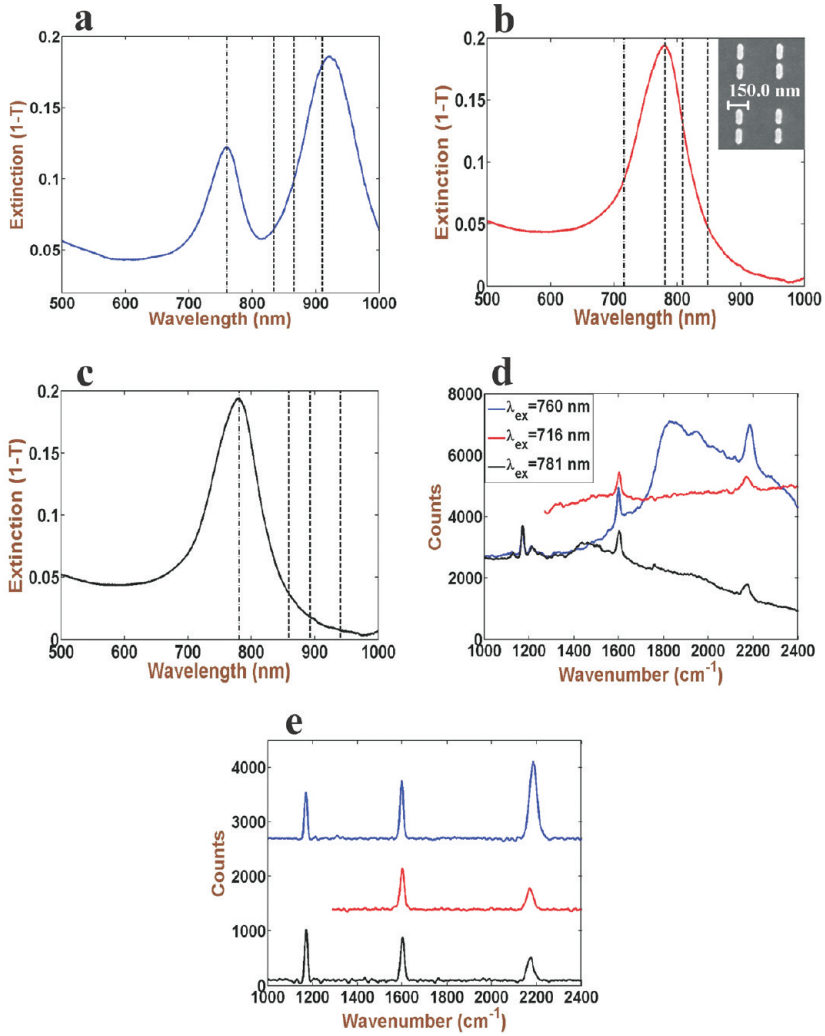

Figure 7. Extinction spectra of (a) mixed ring−rod dimers, and (b and c) of dimer rods. For panels b and c the laser used in the SERS measurement is tuned to 716 and 781 nm, respectively. (d) Measured SERS spectra of mixed and rod dimers. (e) SERS spectra after baseline correction and normalization that accounts for the differences in the laser power and the exposed gold surface areas between the spectra.

From Table 1, it can be seen that, for the 2175 cm^{-1} line, the mixed dimer substrate has an enhancement factor ~3 times larger than the highest enhancement factor of the rod dimer substrate, achieved at an excitation wavelength of 781 nm. The mixed dimer substrate also achieves a ~20% higher enhancement factor for the 1602 cm^{-1} line than the highest rod dimer enhancement factor for that line. Despite the fact that the mixed dimer substrate is optimized for enhancement of the longer wavenumber Stokes lines, its enhancement factor for the 1165 cm^{-1} line is only ~22% smaller than that of the rod dimer substrate. Interestingly, the rod dimers show higher enhancement for 1602 and 2175 cm^{-1} Raman lines when the excitation laser wavelength is 781 nm, rather than 716 nm. This is not in agreement with the result of ref 5 in which the highest enhancement was observed when the excitation laser and Raman lines are at opposite side of the LSPR peak. One possibility is that the near-field enhancement does not exactly follow the far-field enhancement profile of the extinction spectrum in terms of the peak wavelength and its bandwidth.[24]

TABLE 1. Normalized SERS Signal of 1,4-PDI Monolayers on Mixed Dimers and Rod Dimers at Different Excitation Wavelengths

	1165 cm^{-1}	1602 cm^{-1}	2175 cm^{-1}
mixed dimers, λ_{ex} = 760 nm	735	1003	1323
rod dimers, λ_{ex} = 716 nm		582	289
rod dimers, λ_{ex} = 781 nm	940	798	416

In conclusion, surface-enhanced Raman scattering is studied in double-resonance substrates. The experimentally measured SERS enhancement factors are found to be higher for mixed dimers than double dimers. This is in agreement with electromagnetic simulations that indicate that this is due to mixed dimers having stronger spatial overlap between the field distri-

butions occurring at the wavelengths of the laser excitation and of Stokes line. A comparison between the performance of single and double resonance substrates at detecting Stokes lines far from the laser wavelength is performed using 1,4-PDI analyte. The double-resonance substrate, in which resonances are matched to laser and Stokes wavelength at 2200 cm^{-1}, shows a roughly ~3 times stronger SERS enhancement factor than a single-resonance substrate. Future work may involve the use of other nanoparticle shapes[25] or collective effects in nanoparticle arrays[26] to further increase the SERS electromagnetic enhancement factor.

FABRICATION

Gold nanoparticle arrays on glass substrate are fabricated by electron beam lithography and lift off. The starting substrate is a microscope glass slide with a 20 nm thick indium tin oxide (ITO) conduction layer (Sigma Aldrich). A bilayer of PMMA (polymethyl methacrylate), comprising two resists with different molecular weights (495K-A2 and 950K-A2, MicroChem), is formed on the substrate. The electron beam lithography is then carried out with an acceleration voltage of 100 kV, and an area dosage of 1050 $\mu C/cm^2$ on an Elionix ELS7000 system. The substrate is then developed. Next, a gold layer (30 nm) is deposited on the substrate by thermal evaporation. No adhesion layer is used. Lift off is then performed by soaking the substrate in acetone. In Figure 4, scanning electron microscope (SEM) images of the double-resonance structures are shown.

Acknowledgment. This work was supported by the Defense Advanced Research Projects Agency (contract FA9550-08-1-0285). Fabrication was carried out at the Harvard Center for Nanoscale Systems, which is supported by the National Science Foundation. We thank Dr. Paul Peng and Prof. Mazur (Harvard University) for use of their Raman spectrometer.

REFERENCES AND NOTES

1. Maier, S. A.; Atwater, H. A. Plasmonics: Localization and Guiding of Electromagnetic Energy in Metal/Dielectric Structures. *J. Appl. Phys.* **2005**, *98*, 011101/1–10.
2. Hao, E.; Schatz, G. C. Electromagnetic Fields around Silver Nanoparticles and Dimers. *J. Chem. Phys.* **2004**, *120*, 357–366.
3. Kneipp, K. Surface-Enhanced Raman Scattering. *Phys. Today* **2007**, *60*, 40–46.
4. Stiles, P. L.; Dieringer, J. A.; Shah, N. C.; Van Duyne, R. P. Surface-Enhanced Raman Spectroscopy. *Annu. Rev. Anal. Chem.* **2008**, *1*, 601–626.
5. McFarland, A. D.; Young, M. A.; Dieringer, J. A.; Van Duyne, R. P. Wavelength-Scanned Surface-Enhanced Raman Excitation Spectroscopy. *J. Phys. Chem. B* **2005**, *109*, 11279–11285.
6. Chu, Y.; Banaee, M. G.; Crozier, K. B. Double-Resonance Plasmon Substrates for Surface-Enhanced Raman Scattering with Enhancement at Excitation and Stokes Frequencies. *ACS Nano* **2010**, *4*, 2804–2810.
7. Chu, Y.; Crozier, K. B. Experimental Study of the Interaction between Localized and Propagating Surface Plasmons. *Opt. Lett.* **2009**, *34*, 244–246.
8. Papanikolaou, N. Optical Properties of Metallic Nanoparticle Arrays on a Thin Metallic Film. *Phys. Rev. B* **2007**, *75*, 235426/1–7.
9. Liu, N.; Langguth, L.; Weiss, T.; Kästel, J.; Fleischhauer, M.; Pfau, T.; Giessen, H. Plasmonic Analogue of Electromagnetically Induced Transparency at the Drude Damping Limit. *Nat. Mater.* **2009**, *8*, 758–762.
10. Stockman, M. I.; Faleev, S. V.; Bergman, D. J. Localization *versus* Delocalization of Surface Plasmons in Nanosystems: Can One State Have both Characteristics? *Phys. Rev. Lett.* **2001**, *87*, 167401/1–4.
11. Verellen, N.; Sonnefraud, Y.; Sobhani, H.; Hao, F.; Moshchalkov, V. V.; Van Dorpe, P.; Nordlander, P.; Maier, S. A. Fano Resonances in Individual Coherent Plasmonic Nanocavities. *Nano Lett.* **2009**, *9*, 1663–1667.
12. Ikeda, K.; Takase, M.; Sawai, Y.; Nabika, H.; Murakoshi, K.; Uosaki, K. Hyper-Raman Scattering Enhanced by Anisotropic Dimer Plasmons on Artificial Nanostructures. *J. Chem. Phys.* **2007**, *127*, 111103/1–4.
13. Borys, N. J.; Walter, M. J.; Lupton, J. M. Intermittency in Second-Harmonic Radiation from Plasmonic Hot Spots on Rough Silver Films. *Phys. Rev. B* **2009**, *80*, 161407/1–4.
14. Hulteen, J. C.; Young, M. A.; Van Duyne, R. P. Surface-Enhanced Hyper-Raman Scattering (SEHRS) on Ag Film over Nanosphere (FON) Electrodes: Surface Symmetry of Centrosymmetric Adsorbates. *Langmuir* **2006**, *22*, 10354–10364.
15. Synowicki, R. A. Spectroscopic Ellipsometry Characterization of Indium Tin Oxide Film Microstructure and Optical Constants. *Thin Solid Films* **1998**, *313−314*, 394–397.
16. Johnson, P. B.; Christy, R. W. Optical Constants of the Noble Metals. *Phys. Rev. B* **1972**, *6*, 4370–4379.
17. Fang, Y.; Seong, N.; Dlott, D. D. Measurement of the Distribution of Site Enhancements in Surface-Enhanced Raman Scattering. *Science* **2008**, *321*, 388–392.
18. Li, K.; Stockman, M. I.; Bergman, D. J. Self-Similar Chain of Metal Nanospheres as an Efficient Nanolens. *Phys. Rev. Lett.* **2003**, *91*, 227402/1–4.
19. Kappeler, R.; Erni1, D.; Xudong, C.; Novotny, L. Field Computations of Optical Antennas. *J. Comput. Theor. Nanosci.* **2007**, *4*, 686–691.
20. Kneipp, J.; Li, X.; Sherwood, M.; Panne, U.; Kneipp, H.; Stockman, M. I.; Kneipp, K. Gold Nanolenses Generated by Laser Ablation-Efficient Enhancing Structure for Surface Enhanced Raman Scattering Analytics and Sensing. *Anal. Chem.* **2008**, *80*, 4247–4251.
21. LeRu, E. C.; Blackie, E.; Meyer, M.; Etchegoin, P. G. Surface Enhanced Raman Scattering Enhancement Factors: A Comprehensive Study. *J. Phys. Chem. C* **2007**, *111*, 13794–13803.
22. Kim, K.; Shin, D.; Kim, K. L.; Shin, K. S. Electromagnetic Field Enhancement in the Gap Between Au Nanoparticles: The Size of Hot Site Probed by Surface-Enhanced Raman Scattering. *Phys. Chem. Chem. Phys.* **2010**, *12*, 3747–3752.
23. Kim, H. S.; Lee, S. J.; Kim, N. H.; Yoon, J. K.; Park, H. K.; Kim, K. Adsorption Characteristics of 1,4-Phenylene Diisocyanide on Gold Nanoparticles: Infrared and Raman Spectroscopy Study. *Langmuir* **2003**, *19*, 6701–6710.
24. Ross, B. M; Lee, L. P. Comparison of Near- and Far-Field Measures for Plasmon Resonance of Metallic Nanoparticles. *Opt. Lett.* **2009**, *34*, 896–989.
25. Wang, D.; Yang, T.; Crozier, K. B. Charge and Current Reservoirs for Electric and Magnetic Field Enhancement. *Opt. Exp.* **2010**, *10*, 10388–10394.
26. Chu, Y.; Schonbrun, E.; Yang, T.; Crozier, K. B. Experimental Observation of Narrow Surface Plasmon Resonances in Gold Nanoparticle Arrays. *Appl. Phys. Lett.* **2008**, *93*, 181108–181110.